Do Trend Extraction Approaches Affect Causality Detection in Climate Change Studies?

Xu Huang*, Hossein Hassani†, Mansi Ghodsi‡, Zinnia Mukherjee§, Rangan Gupta¶

Abstract

Various scientific studies have investigated the causal link between solar activity (SS) and the earth's temperature (GT). Results from literature indicate that both the detected structural breaks and existing trend have significant effects on the causality detection outcomes. In this paper, we make a contribution to this literature by evaluating and comparing seven trend extraction methods covering various aspects of trend extraction studies to date. In addition, we extend previous work by using Convergent Cross Mapping (CCM) - an advanced non-parametric causality detection technique to provide evidence on the effect of existing trend in global temperature on the causality detection outcome. This paper illustrates the use of a method to find the most reliable trend extraction approach for data preprocessing, as well as provides detailed analyses of the causality detection of each component by this approach to achieve a better understanding of the causal link between SS and GT. Furthermore, the corresponding CCM results indicate increasing significance of causal effect from SS to GT since 1880 to recent years, which provide solid evidences that may contribute on explaining the escalating global tendency of warming up recent decades.

Keywords: Trend extraction approaches; causality detection; Convergent Cross Mapping; sunspot number; global temperature; Singular Spectrum Analysis.

*The Statistical Research Centre, Bournemouth University, Bournemouth University, Bournemouth, 89 Holdenhurst Road, BH8 8EB, UK

†The Statistical Research Centre, Bournemouth University, Bournemouth University, Bournemouth, 89 Holdenhurst Road, BH8 8EB, UK

‡The Statistical Research Centre, Bournemouth University, Bournemouth University, Bournemouth, 89 Holdenhurst Road, BH8 8EB, UK

§Department of Economics, Simmons College, 300 The Fenway, Boston, MA 02115, U.S.A.

¶Department of Economics, University of Pretoria, Pretoria 0002, South Africa

Nomenclature

ADF	Augmented Dickey-Fuller.
CCM	Convergent Cross Mapping.
DF − GLS	Dickey-Fuller test with Generalised Least Squares detrended residuals.
DGT	Detrended global temperature.
EDM	Empirical Dynamic Modeling.
EMD	Empirical Mode Decomposition.
GT	Global temperature.
HEN	Henderson Filter.
HP	Hodrick-Prescott Filter.
KPSS	Kwiatkowski-Phillips-Schmidt-Shin test.
LOESS	Local Regression Filter.
MBA	Model Based Approach.
NP	Ng and Perron test.
PP	Phillips and Perron test.
SIC	Schwarz Information Criterion.
SS	Sunspot number.
SSA	Singular Spectrum Analysis.
WAV	Wavelets Filter.

1   Introduction

Rising global temperature has both short and long term environmental and economic implications. As a result, there is growing interest among scientists worldwide to identify the factors that affect the rate of change in global temperature. The connection between solar activity and global warming has been well established in the scientific literature. For example, see references [1–10]. An indication of solar activity is given by the sunspot number (SS). Sunspots appear as dark spots on the surface of the Sun. Temperatures in the dark centers of sunspots drop to about 3700 K (compared to 5700 K for the surrounding photosphere). They are magnetic regions on the Sun, with the strength of a magnetic field which is thousands of times stronger than the Earth's magnetic field. Sunspots usually come in groups with two sets of spots, namely positive (or north) magnetic field and negative (or south) magnetic field. Sunspots typically last for several days, although very large ones may live for several weeks.[1] The causality between sunspot number (SS) and global temperature has been explored in many scientific work using different causality detection techniques. The data on SS and GT contain many complex dynamic fluctuations. Also, there is a high possibility of the existence of non-stationary features in the data. This poses difficulty in deriving convincing results on causality using parametric techniques. Hence, our motivation for this paper is to provide evidence on the causality between SS and GT using various advanced causality methods [11, 12].

---

[1]Further details can be found at: http://solarscience.msfc.nasa.gov/feature1.shtmlSunspots.

Given the long time series in climate change studies, the detected structural breaks show significant effects on the causality detection outcomes. Also, in [11], we showed that the existing trend of GT can affect causality detection, which may lead to misleading or spurious results for both generally accepted and advanced causality detection methods. This motivates us to investigate the possible effects of the trend on causality detection. We evaluate the differences among various trend extraction techniques and the corresponding effects on the results derived.

In this paper, we adopt a non-parametric causality detection method Convergent Cross Mapping [13]. We use the same dataset of SS and GT, and the corresponding subsamples used in [11, 12]. The analysis uses different representative trend extraction methods covering almost all aspects of trend extraction studies to date and evaluates their corresponding effects on these advanced non-parametric causality tests. The emphasis of this paper is not reviewing all available trend extraction methods. Instead, we focus on the crucial question of whether trend extraction has effects on the advanced causality detection methods and providing comparisons of those effects by a few representative trend extraction methods. To the best of our knowledge, this paper is the first to adopt Convergent Cross Mapping to provide evidence on the causality between sunspot numbers and the global temperature. We contribute to the scientific literature on climate change that focuses on determining the causes of global warming.

The paper is structured as follows: Section 2 briefly introduces both the empirical and advanced causality detection techniques adopted in recent climate change studies; Section 3 provides the descriptive summary of the original and various detrended data considering seven different trend extraction methods; Section 4 summarises and compares the causality detection results by employing different causality detection techniques on the original and various extracted series respectively; Furthermore, Section 5 decomposes both SS and GT into representative components and conducts various causality tests respectively for the comprehensive understanding of the causal link between SS and GT; Finally, Section 6 concludes.

2   Empirical and Advanced Causality Detection Techniques

2.1   Time Domain Granger Causality Test

Granger causality test [14] is the most accepted method for causality analyses and is widely used in a number of disciplines. Various applications and developments of this technique can be found in [15–19]. The regression formulation of Granger causality states that vector X_i is the cause of vector Y_i if the past values of X_i are helpful in predicting the future value of Y_i, two

regressions are considered as follows:

$$X_i = \sum_{t=1}^{T} \alpha_t Y_{i-t} + \varepsilon_{1i}, \tag{1}$$

$$Y_i = \sum_{t=1}^{T} \alpha_t Y_{i-t} + \sum_{t=1}^{T} \beta_t X_{i-t} + \varepsilon_{2i}, \tag{2}$$

where $i = 1, 2, \cdots, N$ (N is the number of observations), T is the maximal time lag, α and β are vectors of coefficients, ε is the error term. The first regression is the model that predicts X_i by using the history of Y_i only, while the second regression represents the model of Y_i is predicted by the past information of both X_i and Y_i. Therefore, if the second model is a significantly better model than the first one, existence of causality is concluded.

2.2 Frequency Domain Causality Test

The frequency domain causality test is the extension of time domain Granger causality test that identifies the causality between different variables for each frequency. In order to briefly introduce the testing methodology, we mainly follow [20, 21]. More details can be found in [22].

It is assumed that two dimensional vector containing X_i and Y_i (where $i = 1, 2, \cdots, N$ and N is the number of observations) with a finite-order Vector Auto-regression Model (VAR) representative of order p,

$$\Theta(R) \begin{pmatrix} Y_i \\ X_i \end{pmatrix} = \begin{pmatrix} \Theta_{11}(R) & \Theta_{12}(R) \\ \Theta_{21}(R) & \Theta_{22}(R) \end{pmatrix} \begin{pmatrix} Y_i \\ X_i \end{pmatrix} + \mathcal{E}_i, \tag{3}$$

where $\Theta(R) = I - \Theta_1 R - ... - \Theta_p R_p$ is a 2×2 lag polynomial and $\Theta_1, ..., \Theta_p$ are 2×2 autoregressive parameter matrices, with $R^k X_i = X_{i-k}$ and $R^k Y_i = Y_{i-k}$. The error vector $\mathcal{E}$ is white noise with zero mean, and $E(\mathcal{E}_i \mathcal{E}_i') = \mathbf{Z}$, where $\mathbf{Z}$ is positive definite matrix. The moving average (MA) representative of the system is

$$\begin{pmatrix} Y_i \\ X_i \end{pmatrix} = \Psi(R) \eta_i = \begin{pmatrix} \Psi_{11}(R) & \Psi_{12}(R) \\ \Psi_{21}(R) & \Psi_{22}(R) \end{pmatrix} \begin{pmatrix} \eta_{1i} \\ \eta_{2i} \end{pmatrix}, \tag{4}$$

with $\Psi(R) = \Theta(R)^{-1} \mathbf{G}^{-1}$ and $\mathbf{G}$ is the lower triangular matrix of the Cholesky decomposition $\mathbf{G}'\mathbf{G} = \mathbf{Z}^{-1}$, such that $E(\eta_t \eta_t') = I$ and $\eta_i = \mathbf{G}\mathcal{E}_i$. The causality test developed in [20] can be written as:

$$C_{X \Rightarrow Y}(\gamma) = log \left[1 + \frac{|\Psi_{12}(e^{-i\gamma})|^2}{|\Psi_{11}(e^{-i\gamma})|^2} \right]. \tag{5}$$

However, according to this framework, no Granger causality from X_i to Y_i at frequency γ corresponds to the condition $|\Psi_{12}(e^{-i\gamma})| = 0$, this condition leads to

$$|\Theta_{12}(e^{-i\gamma})| = |\Sigma_{k=1}^{p} \Theta_{k,12} \cos(k\gamma) - i\Sigma_{k=1}^{p} \Theta_{k,12} \sin(k\gamma)| = 0, \tag{6}$$

where $\Theta_{k,1,2}$ is the $(1,2)th$ element of Θ_k, such that a sufficient set of conditions for no causality is given by [22]

$$\begin{aligned} \Sigma_{k=1}^{p}\Theta_{k,1,2}\cos(k\gamma) = 0 \\ \Sigma_{k=1}^{p}\Theta_{k,1,2}\sin(k\gamma) = 0 \end{aligned}. \tag{7}$$

Hence, the null hypothesis of no Granger causality at frequency γ can be tested by using a standard F-test for the linear restrictions (7), which follows an $F(2, B - 2p)$ distribution, for every γ between 0 and π, with B begin the number of observations in the series.

2.3 Convergent Cross Mapping Technique

Convergent Cross Mapping (CCM) was first introduced in [13] that aimed at detecting the causation among time series and to provide a better understanding of dynamic systems that are well explored by other well established methods such as Granger causality. CCM has proven to be an advanced non-parametric technique for distinguishing causations in a dynamic system that contains complex interactions. More details can be found in [13, 23–25]. We briefly introduce CCM in this paper by following primarily [13].

Assume there are two variables Xi and Yi such that Xi has a causal effect on Yi. CCM will test the causation by evaluating whether the historical record of Yi can be used to get reliable estimates of Xi. We set $i = 1, 2, \cdots, n$. Given a library set of n points that are not necessarily equal to the total number of observations N of two variables, the lagged coordinates are adopted to generate an E-dimensional embedding state space [26, 27], in which the points are the library vector X_i and prediction vector Y_i

$$\begin{aligned} X_i &: \quad \{x_i, x_{i-1}, x_{i-2}, \cdots, x_{i-(E-1)}\}, & (8) \\ Y_i &: \quad \{y_i, y_{i-1}, y_{i-2}, \cdots, y_{i-(E-1)}\}, & (9) \end{aligned}$$

The $E+1$ neighbors of Y_i from the library set X_i will be selected, which actually form the smallest simplex that contains Y_i as an interior point. Accordingly, the forecast is then conducted by this process, which is the nearest-neighbour forecasting algorithm of simplex projection [26]. The optimal E will be evaluated and selected based on the forward performances of these nearby points in an embedding state space.

Therefore, by adopting the essential concept of Empirical Dynamic Modeling (EDM) and generalized Takens' Theorem [27], two manifolds are conducted based on the lagged coordinates of the two variables under evaluation, which are the attractor manifold M_Y constructed by Y_i and respectively, the manifold M_X by X_i. The causation will then be identified accordingly if the nearby points on M_Y can be employed for reconstructing observed X_i. Note that the correlation coefficient ρ is used for the estimates of cross map skill due to its widely acceptance

5

and understanding, additionally, leave-one-out cross-validation is considered a more conservative method and adopted for all evaluations in CCM.

3 Data and Trend Extraction

3.1 Original Data

The GT and SS data are at monthly frequency covering the period from January 1880 to May 2015, with the start and up to date end points being updated based on [11, 12]. The data for GT were obtained from the Goddard Institute for Space Studies (GISS) [28] and the SS data were obtained from the Solar Influences Data Analysis Centre (SIDC) [29]. Figure 1 presents the time series plots of the original variables, in which we can observe the possible existing trend in GT that is addressed with details in [11].

Sunspot Number (SS)   Global Temperature (GT)
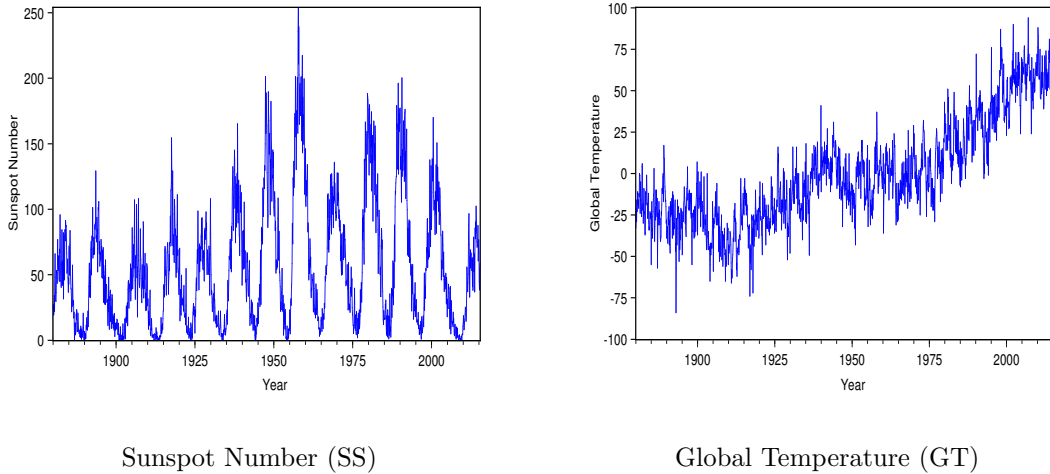
Figure 1: Monthly SS and GT from 1880M01 to 2015M05.

By following [11, 12] with updated data to date, different unit root tests were conducted to verify the stationarity of the series in Table 1. Additionally, structural breaks were detected in the full sample at 1936M03 and 1986M12 by the test proposed in [30] according to [12], whereby the break test was applied to the GT equation of the VAR comprising GT and SS. The test will not be reproduced here (the reader is referred to [12] for details), and all the tests included in this and the following sections will apply for the full sample as well as all sub-samples for comparison.

Table 1: Unit Root Test Results.

Sample Size	Series	Methods	None		Intercept		Intercept and Trend	
			Level	Decision	Level	Decision	Level	Decision
Total Sample (1625 Obs) 1880:1-2015:5	GT	KPSS	———	———	4.234*** (31)	I(1)	0.686***(30)	I(1)
		ADF	-1.301 (17)	I(1)	-1.296 (17)	I(1)	-3.443** (24)	I(0)
		PP	-5.966*** (12)	I(0)	-5.964*** (12)	I(0)	-18.499*** (23)	I(0)
		DF-GLS	———	———	-1.315 (6)	I(1)	-6.639***(3)	I(0)
		NP	———	———	-31.142***(12)	I(0)	-516.032*** (23)	I(0)
	SS	KPSS	———	———	0.464**(15)	I(1)	0.101 (15)	I(0)
		ADF	-2.499**(3)	I(0)	-4.055***(3)	I(0)	-4.109***(3)	I(0)
		PP	-2.526** (14)	I(0)	-3.189** (12)	I(0)	-4.027*** (0)	I(0)
		DF-GLS	———	———	-3.383***(3)	I(0)	-6.879***(3)	I(0)
		NP	———	———	-47.323***(14)	I(0)	-71.585***(14)	I(0)
Sub-sample A (674 Obs) 1880:1-1936:2	GT	KPSS	———	———	0.455*(19)	I(1)	0.430***(19)	I(0)
		ADF	-2.710***(3)	I(0)	-7.207***(2)	I(0)	-7.228***(2)	I(0)
		PP	-4.313***(2)	I(0)	-13.397***(14)	I(0)	-13.424***(14)	I(0)
		DF-GLS	———	———	-6.325***(2)	I(0)	-7.076***(2)	I(0)
		NP	———	———	-234.149***(14)	I(0)	-275.304***(14)	I(0)
	SS	KPSS	———	———	0.053(21)	I(0)	0.051(21)	I(0)
		ADF	-1.819*(3)	I(1)	-3.451***(3)	I(0)	-3.447**(3)	I(0)
		PP	-3.226***(18)	I(0)	-6.075***(8)	I(0)	-6.075***(8)	I(0)
		DF-GLS	———	———	-3.043***(3)	I(0)	-3.322**(3)	I(0)
		NP	———	———	-52.499***(8)	I(0)	-57.985***(8)	I(0)
Sub-sample B (609 Obs) 1936:3-1986:11	GT	KPSS	———	———	0.794***(17)	I(1)	0.321***(16)	I(1)
		ADF	-7.121***(1)	I(0)	-7.211***(1)	I(0)	-7.515***(1)	I(0)
		PP	-12.979***(13)	I(0)	-13.102***(13)	I(0)	-13.678***(13)	I(0)
		DF-GLS	———	———	-3.287***(2)	I(0)	-6.454***(1)	I(0)
		NP	———	———	-92.270***(13)	I(0)	-229.775***(13)	I(0)
	SS	KPSS	———	———	0.061(18)	I(0)	0.052(18)	I(0)
		ADF	-1.690*(2)	I(1)	-2.720*(2)	I(1)	-2.741(2)	I(1)
		PP	-1.932*(11)	I(1)	-3.600***(2)	I(0)	-3.614**(2)	I(0)
		DF-GLS	———	———	-2.718***(2)	I(0)	-2.754*(2)	I(1)
		NP	———	———	-24.056***(2)	I(0)	-24.089***(2)	I(0)
Sub-sample C (342 Obs) 1986:12-2015:5	GT	KPSS	———	———	1.835*** (14)	I(1)	0.083 (13)	I(0)
		ADF	-0.475 (3)	I(1)	-3.410**(3)	I(0)	-7.064***(1)	I(0)
		PP	-1.063 (22)	I(1)	-6.518***(8)	I(0)	-10.546***(9)	I(0)
		DF-GLS	———	———	-0.899 (3)	I(1)	-5.899***(1)	I(0)
		NP	———	———	-15.362***(8)	I(0)	-121.714***(9)	I(0)
	SS	KPSS	———	———	0.464**(15)	I(1)	0.101 (15)	I(0)
		ADF	-0.960 (3)	I(1)	-1.870 (3)	I(1)	-2.229 (3)	I(1)
		PP	-1.526(14)	I(1)	-2.898**(2)	I(0)	-4.027***(0)	I(0)
		DF-GLS	———	———	-1.174(3)	I(1)	-1.427(3)	I(1)
		NP	———	———	-8.847**(2)	I(0)	-11.959 (1)	I(1)

[a] The *, ** and *** indicate significance at the 10%, 5% and 1% respectively.

[b] The critical values are as follows:(1)None: -2.566, -1.941 and -1.616 for ADF and PP at 1%, 5% and 10% level of significance, respectively; (2)Intercept: -3.434, -2.863 and -2.567 (-2.566, 1.941, 1.617) [-13.8, -8.1 and -5.7] {0.739, 0.463, 0.347} for ADF and PP (DF-GLS) [NP] {KPSS} at 1%, 5% and 10% level of significance, respectively;(3)Intercept and Trend: -3.963, -3.412 and -3.128 (3.48, 2.89, 2.57) [-23.80, -17.3 and -14.2] {0.216, 0.146, 0.119} for ADF and PP (DF-GLS) [NP] {KPSS} at 1%, 5% and 10% level of significance respectively.

[c] Numbers in parentheses for ADF, PP and DF-GLS tests indicates lag-lengths selected based on the Schwarz Information Criterion (SIC). For the NP test and the KPSS test, based on the Bartlett kernel spectral estimation method, the corresponding numbers are the Newey-West bandwidth.

Based on our results from the Kwiatkowski-Phillips-Schmidt-Shin (KPSS), augmented Dickey-Fuller (ADF), Dickey-Fuller test with Generalised Least Squares detrended residuals (DF-GLS), Phillips and Perron (PP), and Ng and Perron (NP) unit root tests, the null of a unit root is overwhelmingly rejected (except for KPSS test the null of being stationary, it cannot be overwhelmingly rejected), for the total sample of SS. However, for total sample of GT, while all the tests support that the variable is trend-stationary, the ADF and DF-GLS test tends to suggest non-stationarity of the series when the unit root test-equation has only a constant (or neither a constant and trend in case of the ADF test). The PP and the NP tests, though, indicate stationarity even under the assumption of constant only (and neither a constant and trend in case of the PP test). Given the nature of GT, it is evident that the unit root equation should in fact include a trend. In general, for sub-sample A and sub-sample B we have overwhelming evidence of stationary (especially based on the results of NP test, which have stronger power compared to the other tests [11]). For sample C, while GT is found to be stationary in general at 1% level, the evidence of stationarity, is slightly weaker for SS, barring the PP and NP tests, at 5% level of significance. In summary, for the full sample and all sub-samples, we can conclude that both series are stationary, whilst GT in general is trend-stationary, especially for sub-sample C.

3.2 Trend Extraction Methods and Extracted Data

The detrended GT (DGT) is provided aiming to remove the possible misleading effects of the trend on the causality detection. The objective of this paper is to contribute on finding the solution of whether different trend extraction methods that employed can affect the causality detection in climate change studies. Thus, instead of reviewing all existing trend extraction methods, a few selected and representative trend extraction methods are adopted and compared in this paper by mainly following [31]. The trend extraction methods employed in this paper cover almost all aspects of trend extraction studies to date, including Model Based Approach (MBA), Empirical Mode Decomposition (EMD), Singular Spectrum Analysis (SSA), Wavelet (WAV), Local Regression (LOESS), Henderson Filter (HEN) and Hodrick Prescott Filter (HP). Since our main purpose is not reviewing all trend extraction techniques, we do not reproduce the theoretical introductions of the methods, more details can be found in [31]. The DGT series and corresponding extracted trend series are summarized below in Figure 2 and Figure 3 respectively. Note that all detrended series and corresponding extracted trend series will be adopted for different causality tests respectively with considerations of both total sample and sub-samples in Section 4.
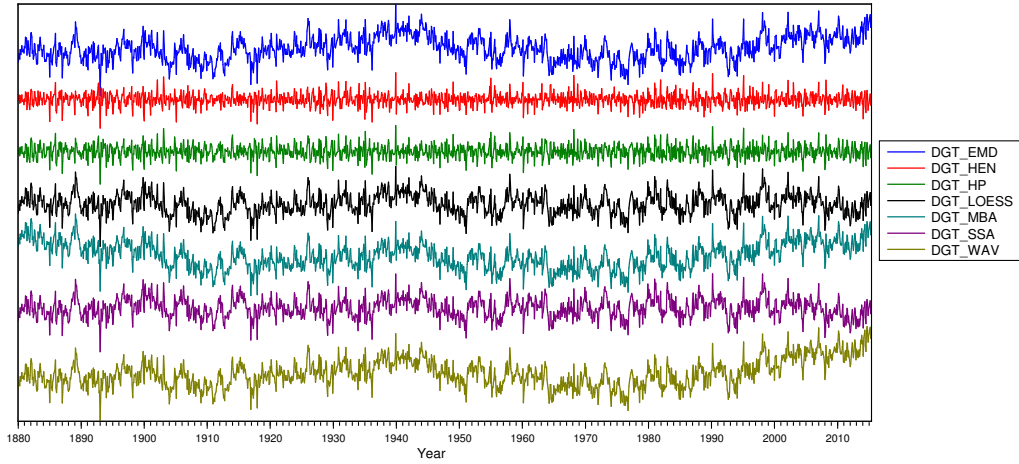
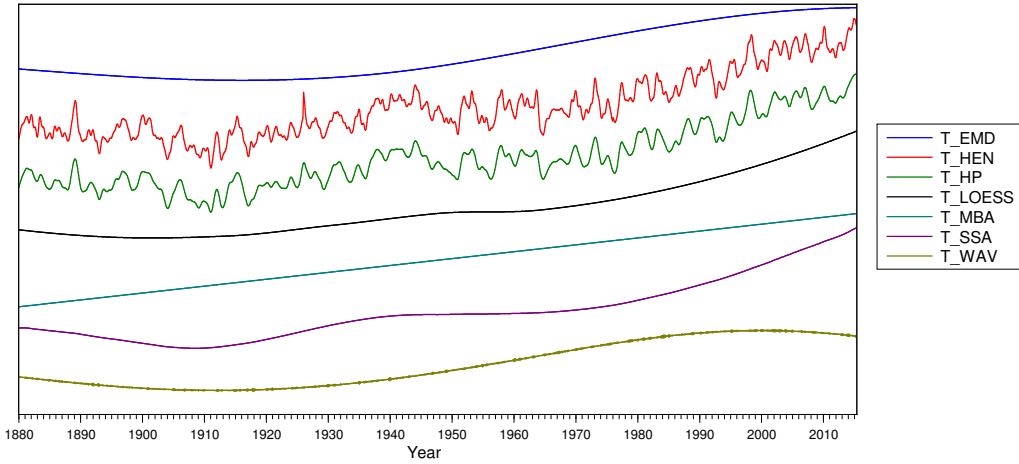Figure 2: Detrended global temperature (DGT) by different methods (1880M01 to 2015M05) .

Figure 3: Extracted trend of global temperature (GT) by different methods (1880M01 to 2015M05) .

4   Causality Test Results of the Original and Extracted Data

Iin this section, the causality tests are conducted for the original series, different detrended series, and extracted trend series respectively. The corresponding results are summarized below by different causality detection techniques.

4.1 Time Domain Causality Test Results

Given the significant and empirical role of time domain causality test, we repeated the Granger causality test with SS and different DGT, as well as extracted trend series by different techniques respectively in Table 2. Note that all tests conducted satisfy the preconditions of time domain causality test with results by the corresponding optimal lag. The null hypothesis that SS does not Granger cause GT in general cannot be rejected for the sub-sample A except for DGT by HEN. The results also point out that the null of non-causality still continued to hold at 5% significant level for all trend and detrended series of sub-sample B and sub-sample C. The overall causality from SS to GT considering the total sample is proved by DGT(HEN), DGT(LOESS) and DGT(SSA) at 5% significant level. Thus, in general, comparing to the insignificant results of the original series, the trend extraction is confirmed helpful on time domain causality test, more specifically, DGT by HEN, LOESS and SSA indicate the significant causal link from SS to GT at the total sample level.

Table 2: Summary of Granger causality test results.

Tested Series	Total Sample 1880:1-2015:5		Subsample A 1880:1-1936:2		Subsample B 1936:3-1986:11		Subsample C 1986:12-2015:5	
	F	p-value	F	p-value	F	p-value	F	p-value
Original	1.0107	0.3642	0.947	0.3884	1.1374	0.3213	1.5871	0.2062
DGT(EMD)	1.9439	0.0842	1.6239	0.1825	1.4771	0.1953	0.6153	0.6055
DGT(HEN)	1.5184	**0.0458**	1.7268	**0.0133**	1.2998	0.2023	0.6559	0.5797
DGT(HP)	1.1439	0.1875	1.4968	0.0522	1.1201	0.2956	0.6757	0.5675
DGT(LOESS)	1.6184	**0.0298**	1.6243	0.1824	2.2294	0.0837	0.6179	0.6039
DGT(MBA)	1.3569	0.2287	1.6244	0.1824	1.4767	0.1955	0.6164	0.6048
DGT(SSA)	1.6201	**0.0295**	1.5080	0.1981	2.2310	0.0835	0.6188	0.6032
DGT(WAV)	1.9514	0.0831	1.6192	0.1836	1.4557	0.2025	0.9852	0.5374
Trend(EMD)	0.6276	0.9689	0.6934	0.9399	0.9475	0.5892	0.5359	0.9499
Trend(HEN)	0.8384	0.6107	1.2114	0.2983	1.1247	0.3212	1.0686	0.4127
Trend(HP)	1.5676	0.1661	0.9720	0.4432	0.9772	0.4309	0.5552	0.6449
Trend(LOESS)	0.5487	0.9552	0.7468	0.7978	0.6677	0.8723	0.4067	0.9527
Trend(MBA)	0.1212	0.9416	0.4413	0.7235	0.4869	0.6147	0.5125	0.6739
Trend(SSA)	0.6943	0.9624	1.2123	0.1642	1.0918	0.3507	0.5151	0.9986
Trend(WAV)	1.5173	**0.0434**	1.2843	0.1547	1.4776	0.0646	1.1989	0.3094

4.2 Frequency Domain Causality Test Results

The frequency domain causality results for the original series are listed below in Figure 4. Note that the optimal lag-structures are maintained for all tests and the test statistics (blue) along with the corresponding 5% critical values (red) for each particular frequencies are adopted to evaluate the possible causal links from SS to GT.
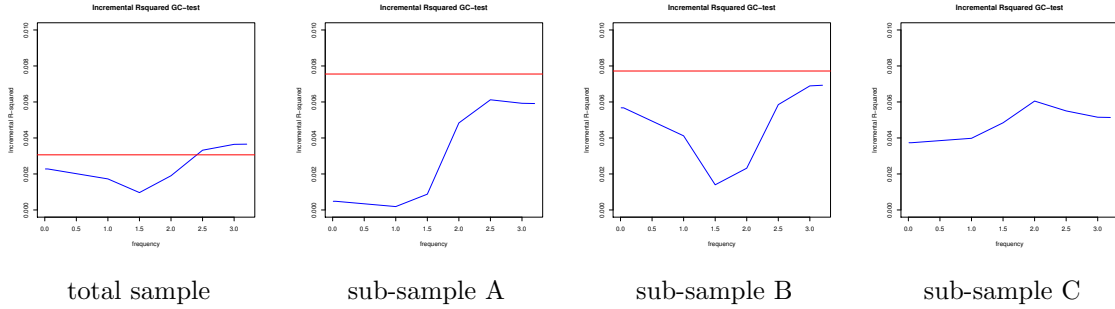
Figure 4: Frequency domain causality result for original GT.

For the full sample, significant causal link is confirmed for frequency that is greater than 2.45 corresponding to a cycle length between 2 and 2.6 months. Whilst, in terms of the sub-samples, no significant causality can be identified for any frequency and the frequency domain test fails to prove that SS has any predictability for GT in the sub-samples.

The following figures present the frequency domain causality test results for DGT by each trend extraction methods respectively with specific results of all sub-samples. Identically, for each test, the optimal lag-structure is assured and having greater test statistics (blue) than the corresponding 5% critical values (red) indicates possible causal links from SS to GT within corresponding frequency range.
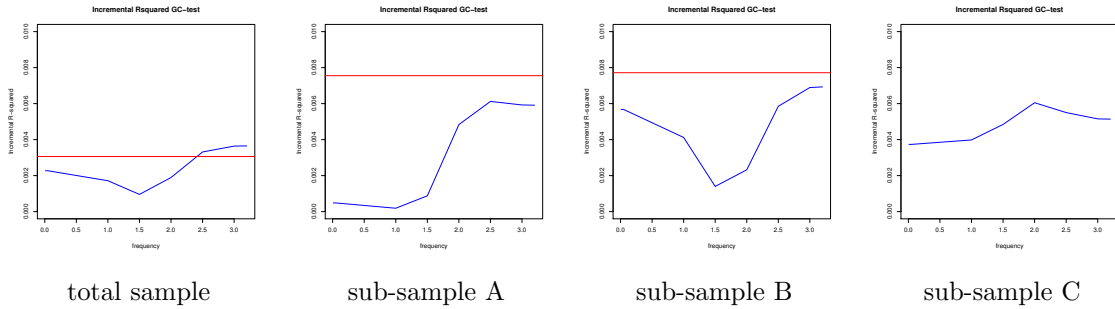
Figure 5: Frequency domain causality result for DGT(MBA).
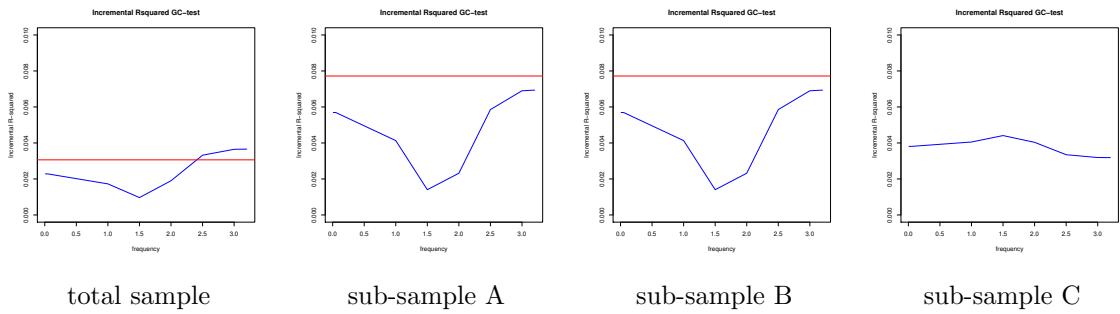
Figure 6: Frequency domain causality result for DGT(EMD).
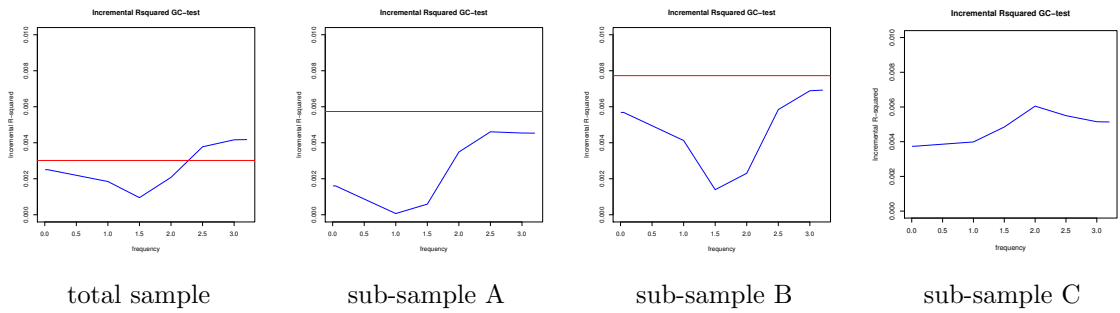
Figure 7: Frequency domain causality result for DGT(SSA).
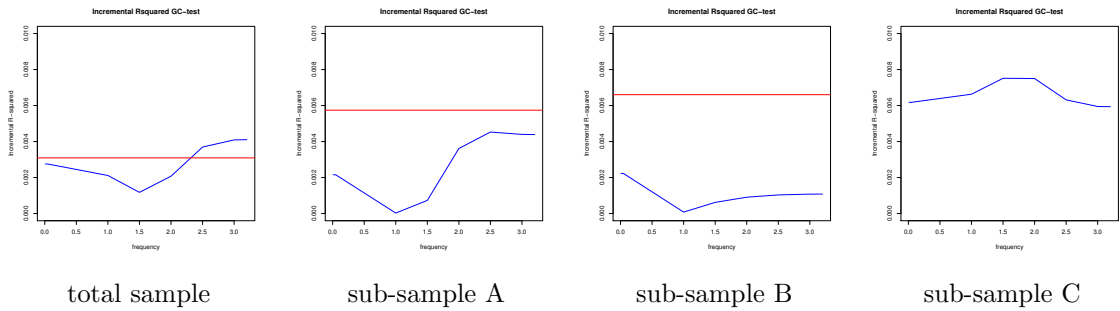
Figure 8: Frequency domain causality result for DGT(WAV).
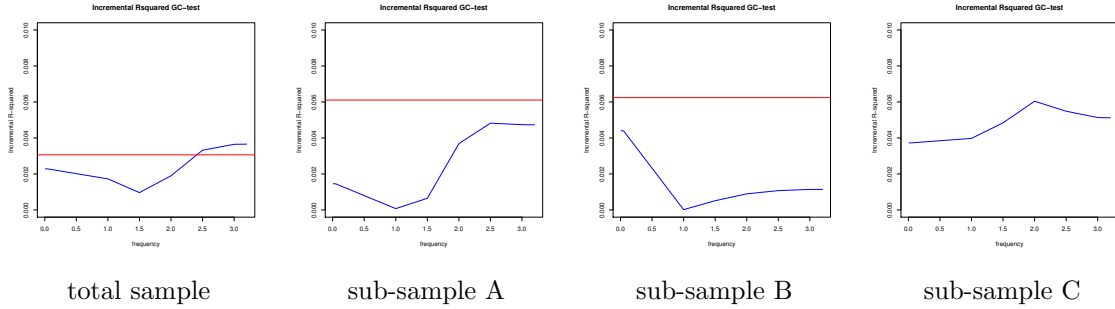
Figure 9: Frequency domain causality result for DGT(LOESS).
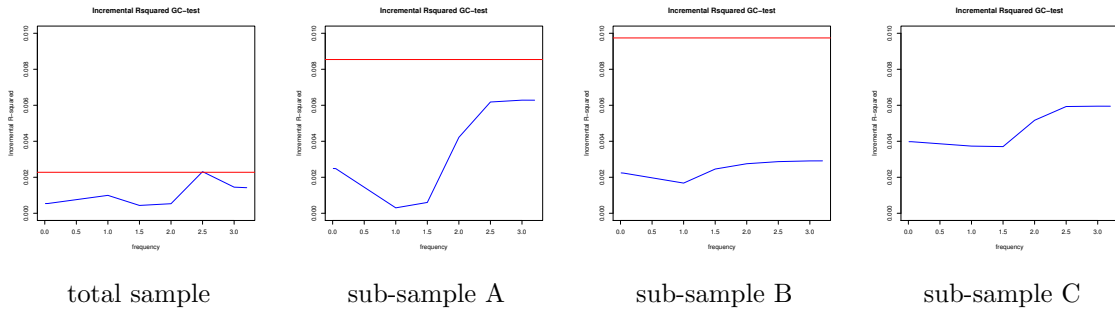
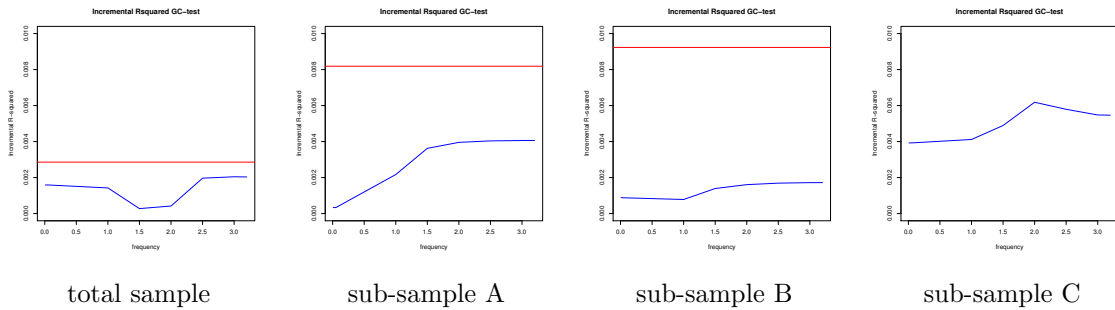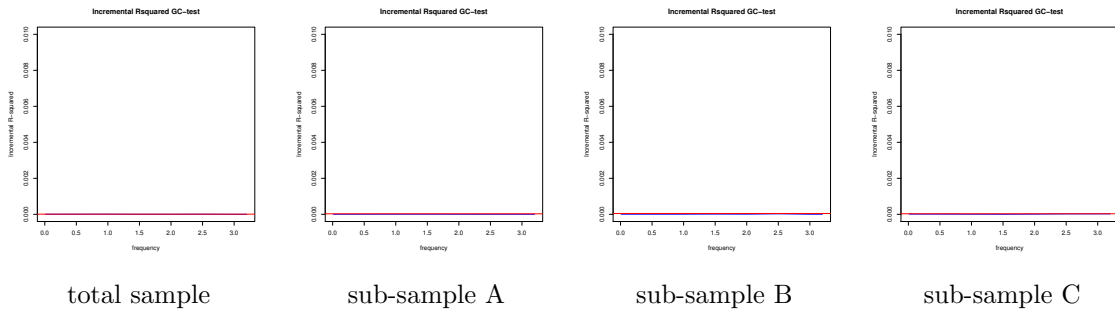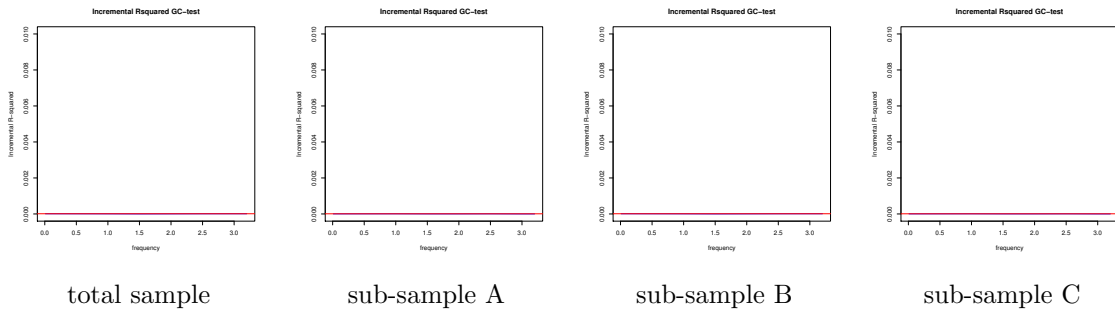Figure 10: Frequency domain causality result for DGT(HEN).

Figure 11: Frequency domain causality result for DGT(HP).

The results of DGT by seven different trend extraction methods above could not reflect significant differences on influencing the frequency domain causality test. In terms of the total sample, weak causality is identified in general except the cases of DGT by HP filter and Henderson filter. The test statistics vary for each trend extraction method considering each sub-sample respectively, however, there are no significant evidences of showing causality for all sub-samples by different trend extraction methods. In general, given the evidences from seven different trend extraction methods adopted, the possible existing trend of GT do not have significant influence on frequency domain causality test and detrending cannot assist or affect significantly on

13

frequency domain causality test for the research of causal link between SS and GT in climate change study.

Furthermore, the following figures present the frequency domain causality test results for trend series extracted by each trend extraction methods respectively with specific results of all sub-samples, followed by the summary of all frequency domain causality test results are listed in Table 3. It is noticed that in general no causality can be detected by the extracted trend series regardless of the sub-samples and trend extraction methods, except that the significant causal link at short cycle frequency is detected at sub-sample B of the trend series extracted by SSA.

| total sample | sub-sample A | sub-sample B | sub-sample C |

Figure 12: Frequency domain causality result for trend(MBA).

| total sample | sub-sample A | sub-sample B | sub-sample C |

Figure 13: Frequency domain causality result for trend(EMD).

| total sample | sub-sample A | sub-sample B | sub-sample C |
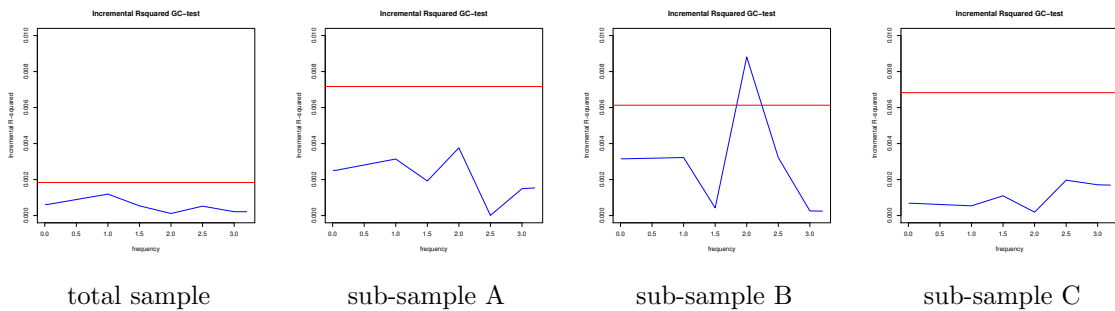
Figure 14: Frequency domain causality result for trend(SSA).

total sample   sub-sample A   sub-sample B   sub-sample C
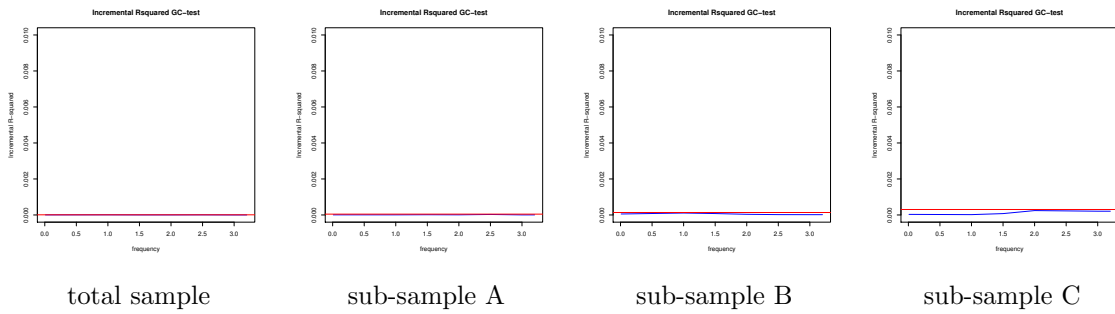
Figure 15: Frequency domain causality result for trend(WAV).

total sample   sub-sample A   sub-sample B   sub-sample C
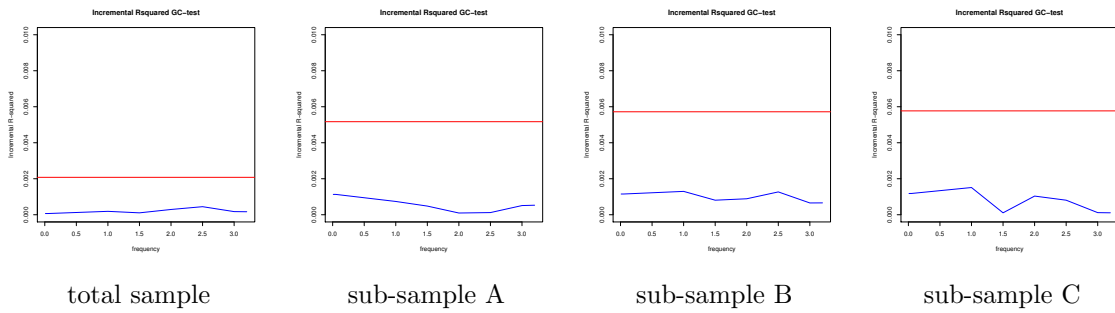
Figure 16: Frequency domain causality result for trend(LOESS).

total sample   sub-sample A   sub-sample B   sub-sample C
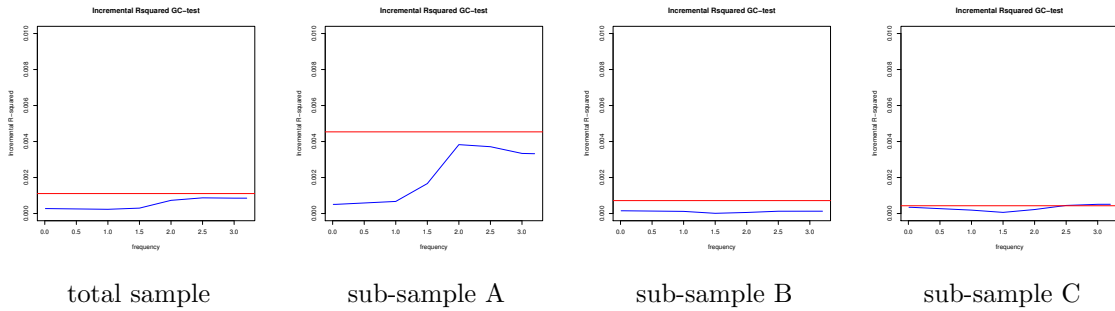
Figure 17: Frequency domain causality result for trend(HEN).

| total sample | sub-sample A | sub-sample B | sub-sample C |
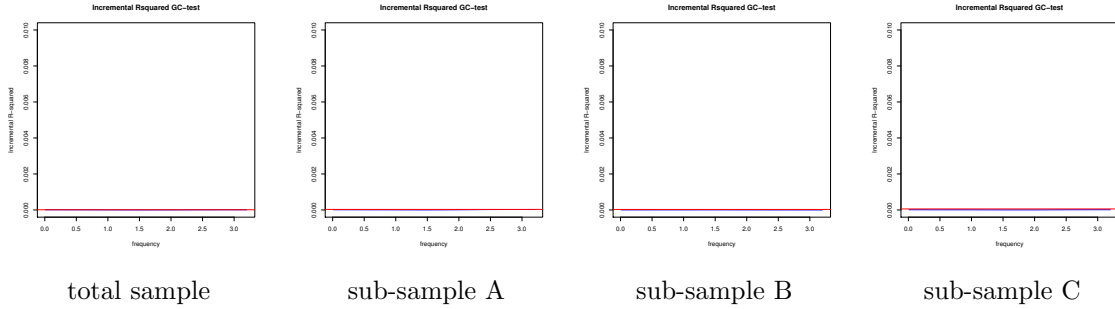
Figure 18: Frequency domain causality result for trend(HP).

Table 3: Summary of frequency domain causality test results.

Tested Series	Total Sample 1880:1-2015:5	Sub-sample A 1880:1-1936:2	Sub-sample B 1936:3-1986:11	Sub-sample C 1986:12-2015:5
Original	YES(short cycle)	NO	NO	NO
DGT(MBA)	YES(short cycle)	NO	NO	NO
DGT(EMD)	YES(short cycle)	NO	NO	NO
DGT(SSA)	YES(short cycle)	NO	NO	NO
DGT(WAV)	YES(short cycle)	NO	NO	NO
DGT(LOESS)	YES(short cycle)	NO	NO	NO
DGT(HEN)	YES(week)	NO	NO	NO
DGT(HP)	NO	NO	NO	NO
Trend(MBA)	NO	NO	NO	NO
Trend(EMD)	NO	NO	NO	NO
Trend(SSA)	NO	NO	YES(short cycle)	NO
Trend(WAV)	NO	NO	NO	NO
Trend(LOESS)	NO	NO	NO	NO
Trend(HEN)	NO	NO	NO	NO
Trend(HP)	NO	NO	NO	NO

4.3 Convergent Cross Mapping Causality Test Results

CCM is adopted for the first time for causality detection analysis in climate change studies, in which the updated data and sub-samples that was used by [11] are employed. It is worth to highlight that the significant advantage of employing this novel non-parametric technique is that no prior linear model assumptions are made and this technique is designed for better understanding of causal relationships in complex dynamical system. Note that all the test results are obtained by the optimal embedding dimension respectively. More specifically, it is determined by the nearest neighbor forecasting performance using simplex projection; Library size is set identical within one corresponding sample size for the sake of further comparisons in the following sections of the paper; Leave-one-out cross validation is applied for the best choice on library size with optimal performance. The results of CCM tests of causation between SS

16

and GT (original) on the whole sample and all sub-samples are listed as follows.

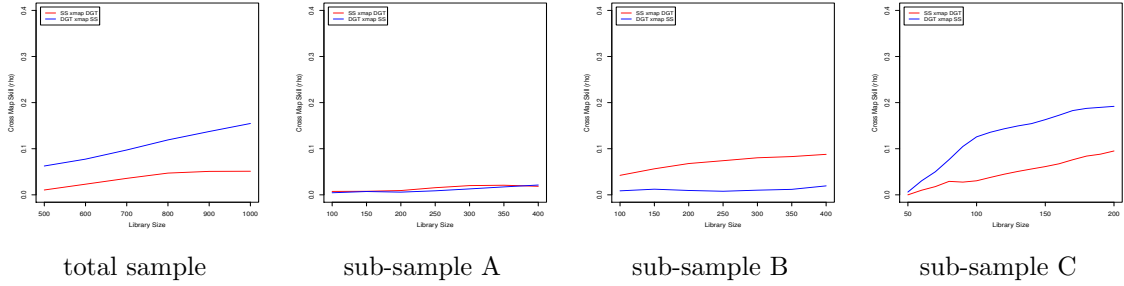| total sample | sub-sample A | sub-sample B | sub-sample C |

Figure 19: CCM result for original GT.

The cross map skill index reflects the reconstruction ability of the fact factor to the cause factor for both directions respectively. Therefore, according to the CCM results of the original series, CCM indicates significant ability of cross mapping considering the total sample, in which, positive outcome reflects identified causal link from SS to GT. However, regarding each sub-sample, sub-sample A cannot detect obvious causation from SS to GT; sub-sample B show opposite causation from GT to SS, which is considered misleading results due to the fact; sub-sample C reflects significant causation from SS to GT that possibly contains the influence of trend. Note that due to the long time span of the data and the wide scale of library size considered for more comprehensive analyses and comparisons, the increasing significance level along with larger library size is reasonable as more information is adopted for cross validation test and then for cross mapping.

Following the CCM test for original series, the figures listed below show all the CCM test results for DGT by different trend extraction methods. Identically, all tests are obtained by the optimal embedding dimension respectively; by optimal outcome based on cross validation results; with identical library size within one corresponding sample size for the sake of comparisons.
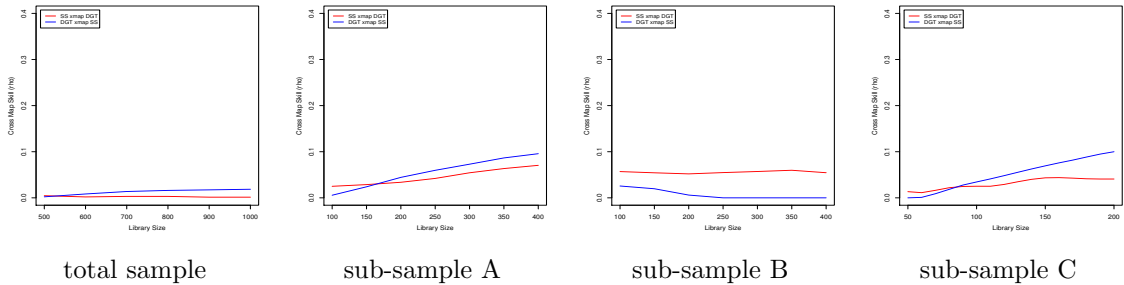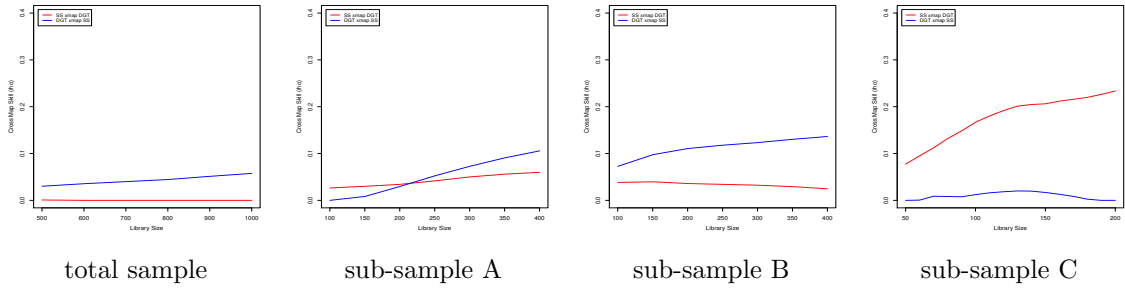

| total sample | sub-sample A | sub-sample B | sub-sample C |

Figure 20: CCM result for DGT(MBA).

17

total sample   sub-sample A   sub-sample B   sub-sample C

Figure 21: CCM result for DGT(EMD).

total sample   sub-sample A   sub-sample B   sub-sample C
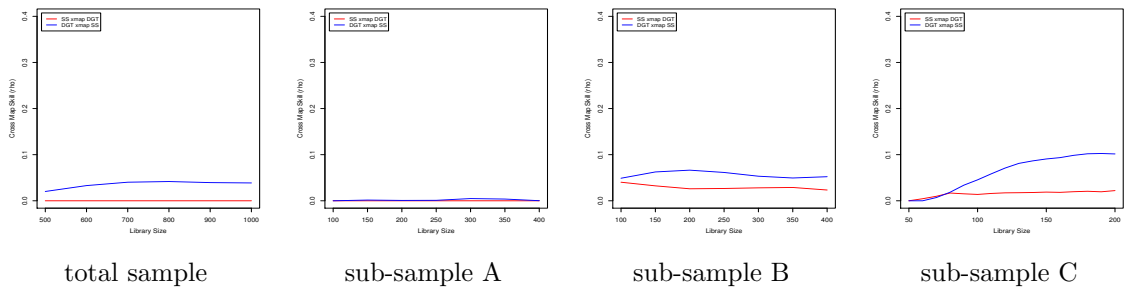
Figure 22: CCM result for DGT(SSA).

total sample   sub-sample A   sub-sample B   sub-sample C
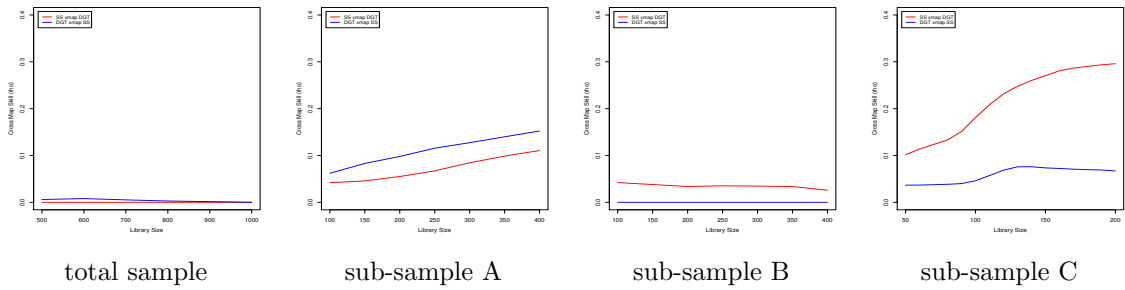
Figure 23: CCM result for DGT(WAV).

total sample   sub-sample A   sub-sample B   sub-sample C
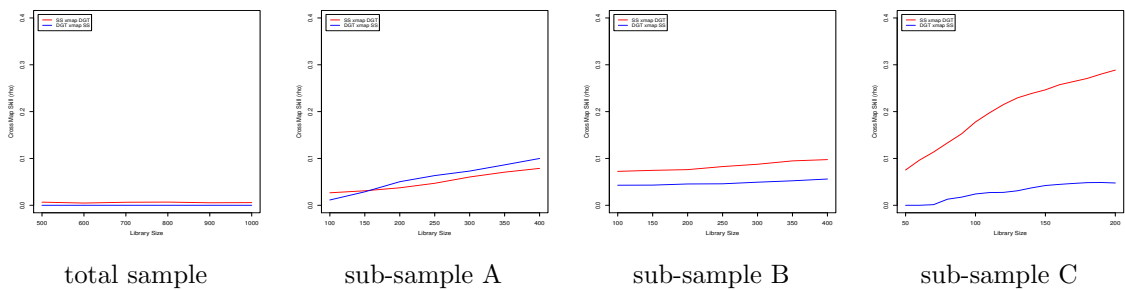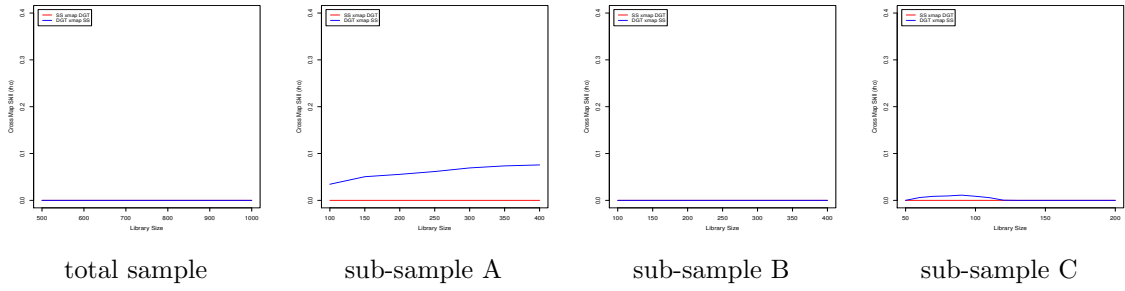
Figure 24: CCM result for DGT(LOESS).
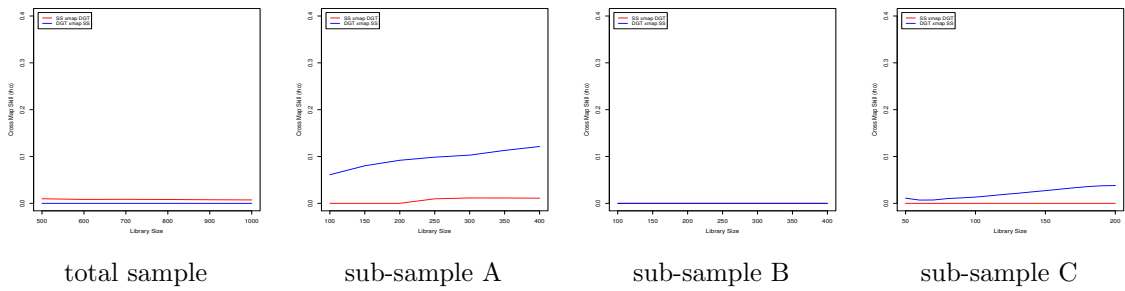
Figure 25: CCM result for DGT(HEN).

Figure 26: CCM result for DGT(HP).

Furthermore, the figures listed below show all the CCM test results for trend series extracted by different trend extraction methods respectively with considerations of both total sample and sub-samples.
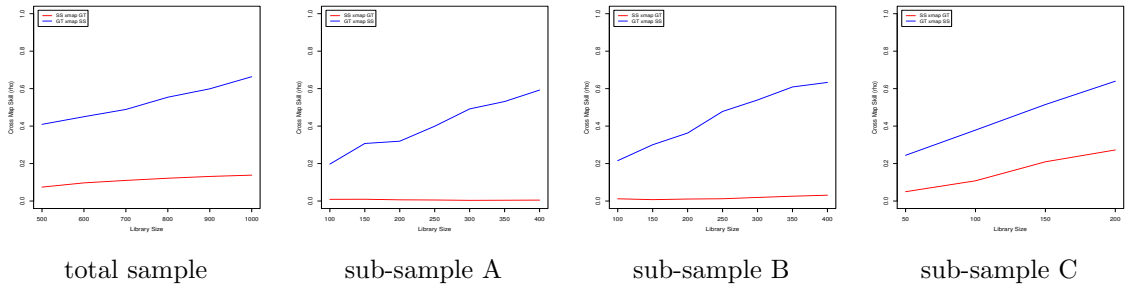

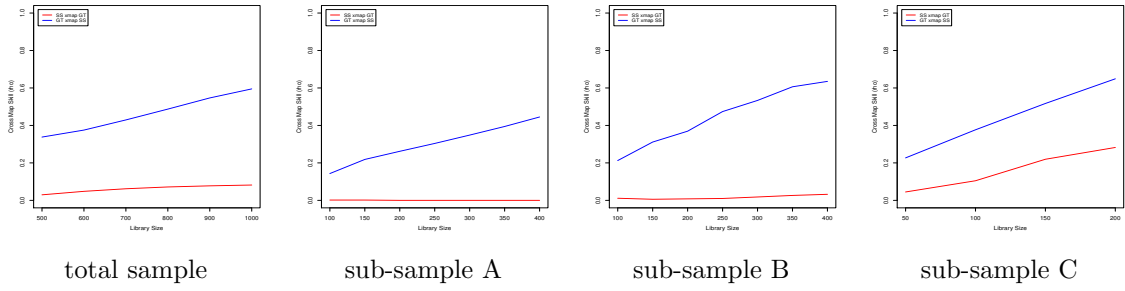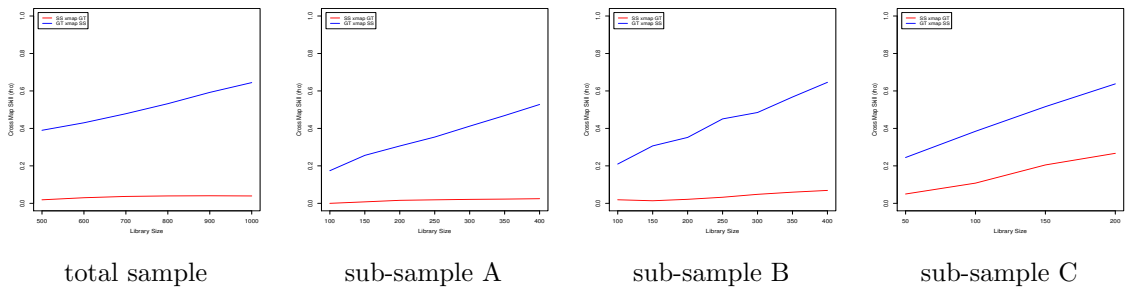Figure 27: CCM result for trend(MBA).

total sample   sub-sample A   sub-sample B   sub-sample C

Figure 28: CCM result for trend(EMD).

total sample   sub-sample A   sub-sample B   sub-sample C

Figure 29: CCM result for trend(SSA).

total sample   sub-sample A   sub-sample B   sub-sample C
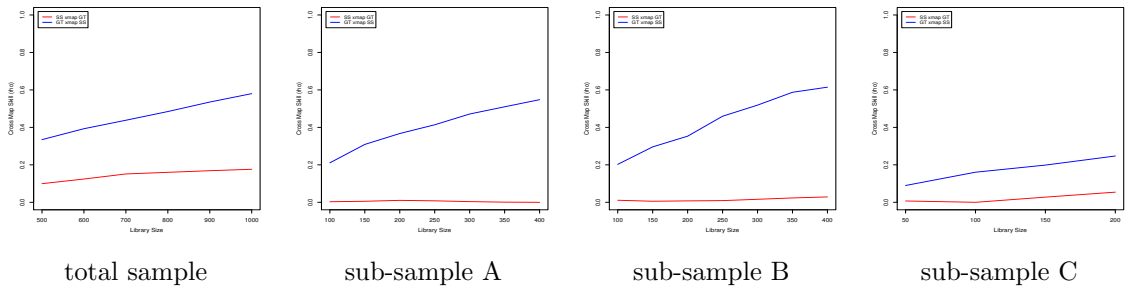
Figure 30: CCM result for trend(WAV).

total sample   sub-sample A   sub-sample B   sub-sample C
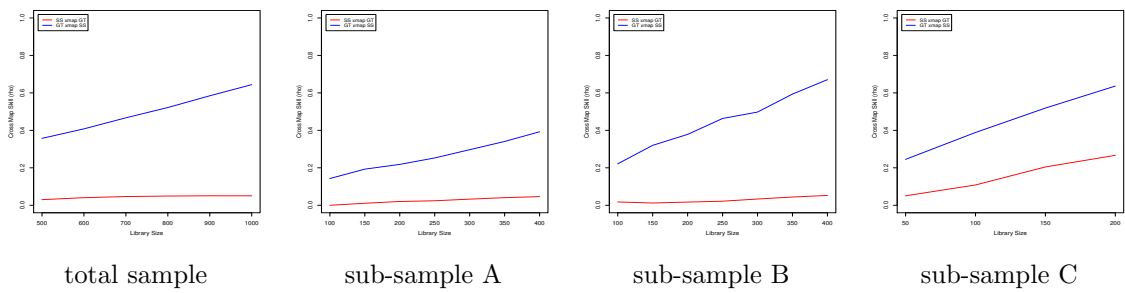
Figure 31: CCM result for trend(LOESS).

total sample   sub-sample A   sub-sample B   sub-sample C

Figure 32: CCM result for trend(HEN).

total sample   sub-sample A   sub-sample B   sub-sample C
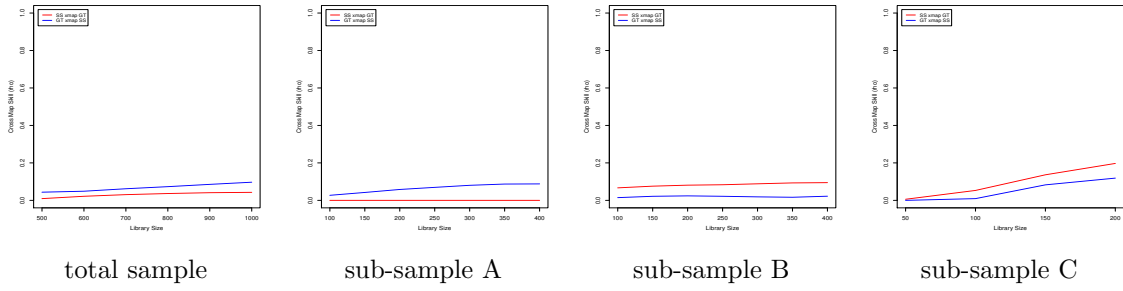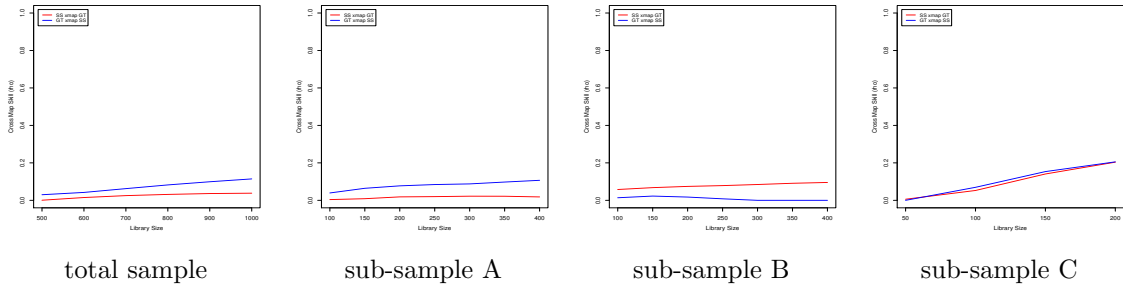
Figure 33: CCM result for trend(HP).

If the CCM results of original GT are recalled for comparison, in which, the total sample and sub-sample C both indicate significant causation from SS to GT, whilst sub-sample A reflects no causation and sub-sample B shows wrong direction. In terms of the DGT and trend series in line with the corresponding CCM results listed above, significant differences are generally obtained among seven different trend extraction methods. In order to provide further analyses on the corresponding effects of each trend extraction method on CCM causality test, the results are again summarized to be more brief below in Table 4.

We find evidence of significant causality in general in terms of trend series, which strongly reflect the causal link from SS to the emerging trend of global warming. Only trend by HP and HEN show relatively weaker causality, while the corresponding DGT by HEN and HP also fail on providing positive results of existing causal links. However, regarding the total sample that was proved significant by original series, DGT (as well as trend series) by MBA, EMD, SSA and WAV continue to hold significant results. Thus, DGT by LOESS, HEN and HP may work fine on extracting the existing trend, but it will possibly remove or reduce the causal effects between SS and GT to be captured by CCM.

Regarding the sub-sample A, all CCM results in general show significant evidences of causality, regardless of whether the level of causation is weak or strong. This is an impressive effect detected as no causal link can be identified when the original series are considered. We can conclude that the existing trend series and DGT together lead to weaken or mislead the results for

Table 4: Summary of CCM causality test results.

Tested Series	Total Sample 1880:1-2015:5	Sub-sample A 1880:1-1936:2	Sub-sample B 1936:3-1986:11	Sub-sample C 1986:12-2015:5
Original	YES	NO	Wrong Direction	YES
DGT(MBA)	YES(very weak)	YES(weak)	Wrong Direction	YES(weak)
DGT(EMD)	YES	YES(weak)	YES	Wrong Direction
DGT(SSA)	YES	YES(very weak)	YES	YES
DGT(WAV)	YES(very weak)	YES	Wrong Direction	Wrong Direction
DGT(LOESS)	NO	YES(weak)	Wrong Direction	Wrong Direction
DGT(HEN)	NO	YES	NO	YES(very weak)
DGT(HP)	NO	YES	NO	YES(weak)
Trend(MBA)	YES(strong)	YES(strong)	YES(strong)	YES(strong)
Trend(EMD)	YES(strong)	YES(strong)	YES(strong)	YES(strong)
Trend(SSA)	YES(strong)	YES(strong)	YES(strong)	YES(strong)
Trend(WAV)	YES(strong)	YES(strong)	YES(strong)	YES
Trend(LOESS)	YES(strong)	YES	YES(strong)	YES(strong)
Trend(HEN)	YES(week)	YES(week)	Wrong Direction	Wrong Direction
Trend(HP)	YES(week)	YES(week)	Wrong Direction	YES(very week)

sub-sample A on causality analyses. This can be generally improved to obtain more significant outcomes by extracting the trend with all representative trend extraction methods listed here (regardless the level of significance for different methods).

In terms of sub-sample B, which indicated a wrong direction causality in case of the original series, only DGT by EMD and SSA show positive results indicating causality. The others fail to detect or, even worse, provide misleading results of wrong direction of causation.

For the most recent sub-sample C that possibly reflects the most meaningful conclusion, DGT by SSA manage to hold the significant result that keep the consistency of the results by original series, more importantly, with reasonable level of significance. In more details, the CCM results of DGT by SSA show emerging causality relationship from SS to GT that also prove the significant predictive ability of SS on GT.

As an advanced non-parametric causality detection method, CCM outperforms the other generally accepted methods with not only the original series but also the DGT and extracted trend series. However, the existing trend of GT has also been proved affecting the outcomes of CCM. According to the comparisons of different trend extraction methods in terms of the study of SS and GT in climate change, SSA outperforms the others on providing better preprocessed series for CCM test with significant causal link detected regardless of the DGT and trend series for all sub-samples as well as the total sample. More importantly, it indicates the emerging causal effects from SS to GT, which contributes on explaining the tendency of global warming recent decades.

5 Data Decomposition by SSA and Effects on Causality Detection

All previous comparisons are conducted by the original SS together with the trend and DGT respectively, in line with the SSA technique is found the most appropriate trend extraction method on data preprocessing for causal analyses in climate change study. In this section, both the SS and GT are further decomposed by SSA into representative components: trend, cycle and noise. All causality tests are then obtained by different components respectively to provide further comprehensive understanding of the causal link between SS and GT, which may contribute on target the most significant component that dominates the causal analysis in a complex system like climate changes study.

5.1 Singular Spectrum Analysis Technique

Singular Spectrum Analysis (SSA) is a relatively new and advanced technique of time series analysis. It is stated as a nonparametric technique incorporating the elements of classical time series analysis, multivariate statistics, multivariate geometry, dynamical systems, and signal processing [32]. More coherent, detailed explanations and various applications of both standard SSA and its multivariate extension – MSSA can be found in ([33–42]). The SSA technique is performed in two stages, which are known as decomposition and reconstruction. Embedding and Singular Value Decomposition (SVD) are included in the first stage of decomposition, while the second phase of reconstruction contains grouping and diagonal averaging. Brief descriptions of SSA steps classified by the structure state of the matrix are listed below.

Step 1: Embedding. The one-dimensional time series $Y_N = (y_1, \ldots, y_N)$ is firstly transferred into the multi-dimensional series $X_1, \ldots, X_K$ with vectors $X_i = (y_i, \ldots, y_{i+L-1})^T \in \mathbf{R}^L$, where $L(2 \leq L \leq N-1)$ is the window length and $K = N - L + 1$. The result of this step is the trajectory matrix $\mathbf{X} = [X_1, \ldots, X_K] = (x_{ij})_{i,j=1}^{L,K}$.

Step 2: SVD. Here we perform the SVD of $\mathbf{X}$. Denote by $\lambda_1, \ldots, \lambda_L$ the eigenvalues of $\mathbf{XX}^T$ arranged in the decreasing order $(\lambda_1 \geq \ldots \geq \lambda_L \geq 0)$ and by $U_1 \ldots U_L$ the corresponding eigenvectors. The SVD of $\mathbf{X}$ can be written as $\mathbf{X} = \mathbf{X}_1 + \ldots + \mathbf{X}_L$, where $\mathbf{X}_i = \sqrt{\lambda_i} U_i V_i^T$.

Step 3: Grouping. The grouping consists in splitting the elementary matrices into several groups and summing the matrices within each group.

Step 4: Diagonal averaging. This step aims at transforming a matrix to the form of a Hankel matrix, which can be subsequently converted back to a time series.

5.2 Data Decompositions by SSA

As can be seen in Figure 34 and Figure 35, the original GT and SS are decomposed by SSA into the representative components of trend, cycle and noise respectively. Note that the window

length is selected as $N/2$ where N is the number of observations. All operations are conducted by R with the corresponding package (RSSA)[2].
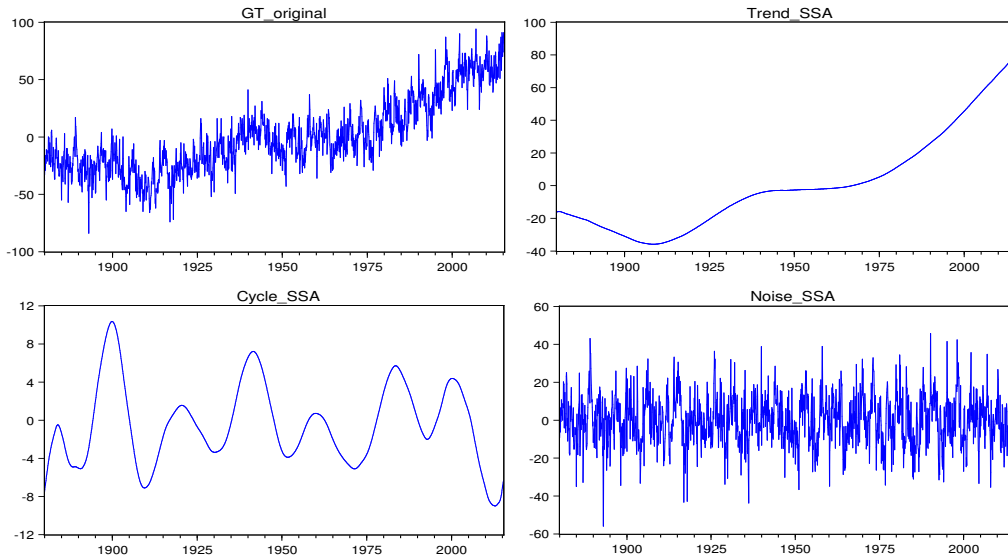

Figure 34: Decompositions of global temperature (DGT) by SSA (1880M01 to 2015M05) .
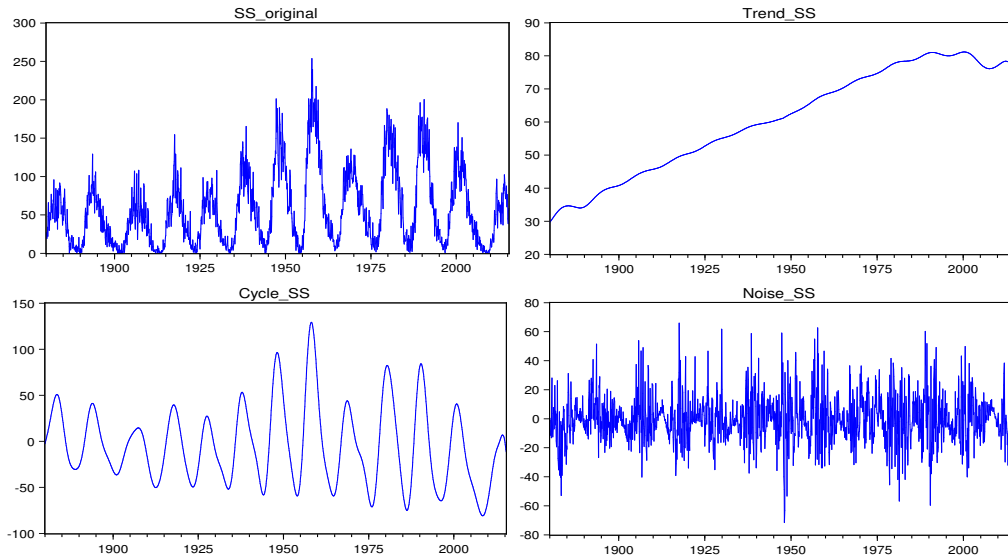

Figure 35: Decompositions of sunspot number (SS) by SSA (1880M01 to 2015M05) .

---

[2]Combinations of eigenvalues are selected due to the features of representative components (further details are available upon request from the authors). Also, there are different alternative packages available in R, as well as another software CaterpillarSSA

5.3 Causality Test Results of the Data Decompositions by SSA

The causality tests are conducted on each group of components respectively with considerations of not only the total sample but also all sub-samples. The detailed results of frequency domain and CCM tests are listed below, followed by the brief summary of causality test results by components in Table 5.
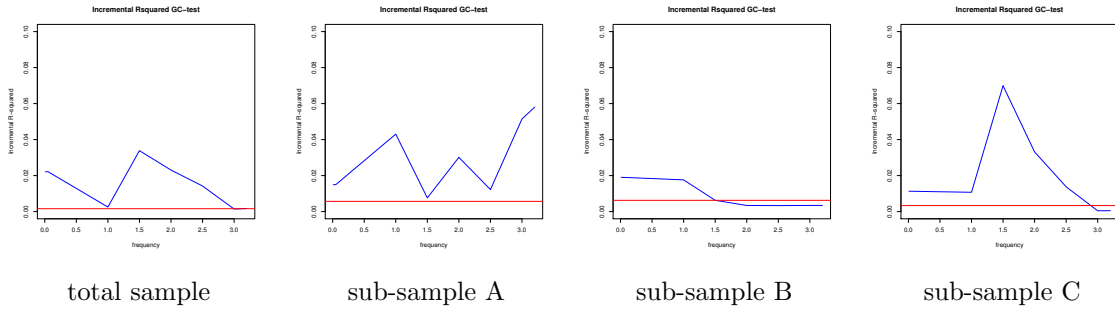

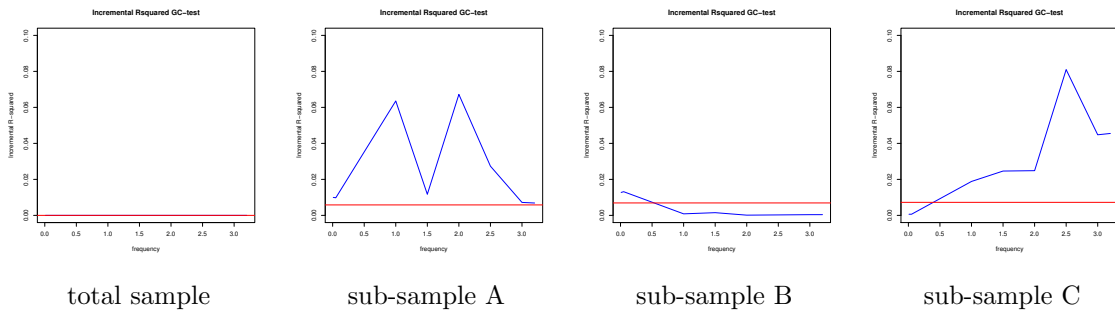Figure 36: Frequency domain causality result for trends.

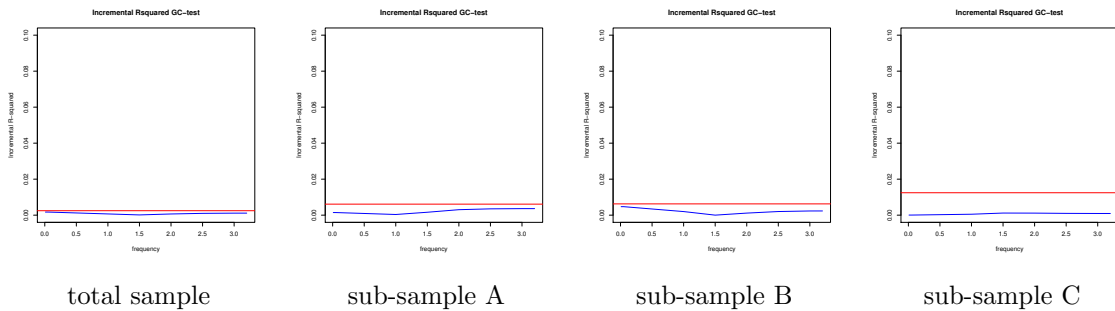Figure 37: Frequency domain causality result for cycles.

Figure 38: Frequency domain causality result for noises.

25
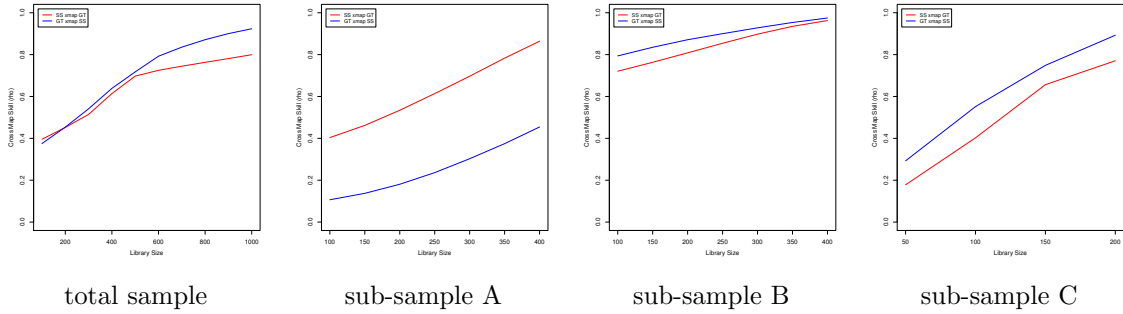
Figure 39: CCM causality result for trends.
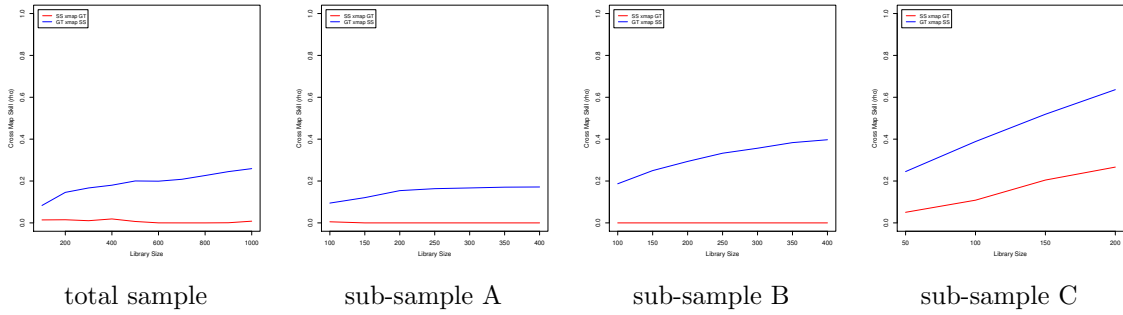
Figure 40: CCM causality result for cycles.
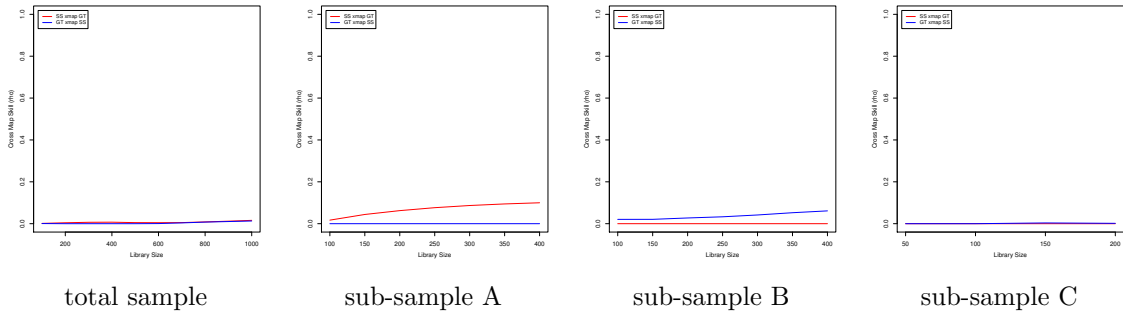
Figure 41: CCM causality result for noises.

6   Discussion

When we decompose the data into different components, we find that even the generally accepted
parametric method time domain causality test achieves the significant results for both trend
and cycle series (except for the sub-sample B of the cycle component). For the frequency domain
and CCM causality tests, the significant causal link is generally proved significant for both the
trend and cycle series. Only the total sample of cycle fails to be detected by frequency domain

Table 5: Summary of causality test results of decomposed data by SSA.

	Decomposition	Total Sample 1880:1-2015:5	Sub-sample A 1880:1-1936:2	Sub-sample B 1936:3-1986:11	Sub-sample C 1986:12-2015:5
	Trend	YES(5.2009***)	YES(8.5674***)	YES(4.4397***)	YES(3.3258***)
Time Domain	Cycle	YES(11.5135***)	YES(7.6866***)	NO(0.9371)	YES(9.7739***)
	Noise	NO(1.7220)	NO(0.9646)	NO(1.5214)	NO(0.4616)
	Trend	YES	YES	YES	YES
Frequency Domain	Cycle	NO	YES	YES	YES
	Noise	NO	NO	NO	NO
	Trend	YES(week)	Wrong Direction	YES(week)	YES
CCM	Cycle	YES	YES	YES	YES
	Noise	NO	Wrong Direction	YES(week)	NO

test, and sub-sample A of trend component shows misleading results of opposite direction of causation by CCM. The causality is overwhelmingly rejected for the noise component by both time domain and frequency domain tests, except the sub-sample B by CCM test. In case of the trend component, the overall significant results indicate the long term causal effect from SS to GT, while the CCM results provide comprehensive analyses that the predictive ability from the other direction is also relatively strong. This is due to the feature of the component and it is worth highlighting that the results by CCM (considering the gap between two cross mapping skill indices) reflect the wrong direction - very weak SS to GT - slightly stronger SS to GT across the sub-samples in line with week causation detected over the total sample.

In terms of the cycle component, the results by different causality tests are generally significant. We find that no causality can be detected by time domain test in sub-sample B. The corresponding results by frequency domain test is also weak (only in limited range of long cycle). CCM is the most sensitive technique that shows the highly significant causality of sub-sample B comparing to the other tests. It is worthwhile to note that the week causality detected by CCM on the noise component at sub-sample B. This possibly indicates some irregular or nonlinear patterns of causal relationships that is also successfully captured by CCM. More importantly, in case of the CCM results of the cycle component across the time scale, we again prove the emerging causal effects of SS on GT. This indicates the tendency of global warming due to sunspot activity, especially for the recent decades.

In general, by decomposing the data into representative components with SSA technique, even the applicability of the basic parametric method (time domain causality test) is significantly improved. The causal link conclusion is overwhelmingly obtained, while the CCM shows the strongest ability of capturing the possible causal effects regardless of the time scale and components. The data preprocessing is absolutely necessary for the causal analyses of the complex system like climate change, and it has been proved to be able to significantly improve the performances of generally all causality tests.

7 Conclusion

In this paper, we analyze the possible effects of the existing trend on causality detection technique performances. Specifically, we use data on sunspots and global temperature, used to climate change studies, to test causality with the empirical time domain causality test as well as advanced non-parametric causality detection techniques such as domain causality test and CCM. This is the first paper to apply CCM to find evidence on the causal relationship between SS and GT. Previous work [11,12] illustrated that these non-parametric methods outperformed the generally accepted techniques of investigating the causal link between SS and GT by showing significant advantages on analyzing data with nonlinear features or complex fluctuations. We extend this literature by conducting various well-established trend extraction methods and evaluating the possible effects on the causality detection in climate change study. For the first time, we provide evidence on the emerging significant predictive ability of SS on GT and, more importantly, the reconstruction ability of using extracted information from fact factor on the cause factor based on information theory. CCM is demonstrated to be a reliable method for causality detection in climate change study with outstanding performances in complex systems.

When we compare the different effects of the existing trend of GT with seven mainstream trend extraction methods, we find that the frequency domain causality test do not get significant influences by existing trend. The weak causality continues to hold for the total sample among DGT by different trend extraction methods, and there are no significant differences captured among causal analyses across sub-samples by preprocessing the data with different methods (except the week short cycle causality detected on trend extracted by SSA in sub-sample B).

Conversely, the outcomes of CCM causality test varies when different trend extraction techniques are considered. It is recognized that all trend extraction methods can improve the causality analyses for sub-sample A, which previously was led to either wrong or misleading results by the existing trend. DGT by LOESS, HEN and HP can possibly remove or reduce the causal effects between SS and GT to be clearly captured for the total sample. Only DGT by EMD and SSA get positive results indicating causality for sub-sample B, while the others show misleading direction of causality or fail to identify any. Last and most import sub-sample C, which reflects the results of most recent decades, only DGT by SSA manage to hold the significant result. Additionally, DGT by SSA shows the emerging causality relationship from SS to GT across all sub-samples. This confirms the strong causal relationship between SS and GT, also contributes to providing convincing evidence on the emerging global warming. SSA is therefore proved the most appropriate trend extraction technique for data preprocessing aiming at providing better causal analyses of SS and GT.

Furthermore, the data is decomposed by SSA into representative components of trend, cycle and noise, which proves to contribute on achieving the significant improvements on the performances of all causality tests, even the parametric time domain causality test. The causality is overwhelmingly confirmed regardless of the component and time scale, and CCM shows the

strongest ability and sensitivity of capturing possible causal links between SS and GT.

This paper successfully answers a crucial question that the existing trend has impacts on the causality analyses outcomes, even for the advanced non-parametric techniques that already outperformed the generally accepted methods with significant advantages. We also confirm that trend extraction will absolutely contribute on assisting the causal analyses in climate change study, whilst the causality analyses will still lead to conclusions with great contrast by using different trend extraction methods. Among which, the SSA trend extraction is identified as the most reliable method for data preprocessing, while CCM shows outstanding performance among all causality tests adopted. The emerging causal effects from SS to GT, especially for recent decades, are overwhelmingly proved, which reflects the better understanding of the tendency of global warming.

Broadly, this paper contributes to the scientific literature on climate change in various ways. It provides a better process of causal analyses on a complex system like climate change study and identifies the most reliable trend extraction method for data preprocessing to study causality between SS and GT. It provides a comprehensive analysis of the causal effects by different components and demonstrates CCM as the most reliable causality detection technique due to its robust performances on not only the dominating components like trend and cycle but also the less important component of noise.

References

[1] J.L. Lean and D.H. Rind. Climate forcing by changing solar radiation *Journal of Climate*, 11(12): 3069–3094, 1998.

[2] J.L. Lean and D.H. Rind. How will Earth's surface temperature change in future decades? *Geophysical Research Letters*, 36(15), 2009. Wiley Online Library. [DOI: 10.1029/2009GL038932]

[3] N. Scafetta Empirical evidence for a celestial origin of the climate oscillations and its implications. *Journal of Atmospheric and Solar-Terrestrial Physics*, 72(13): 951–970, 2010.

[4] N. Scafetta A shared frequency set between the historical mid-latitude aurora records and the global surface temperature. *Journal of Atmospheric and Solar-Terrestrial Physics*, 74: 145–163, 2012.

[5] N. Scafetta and P. Grigolini and T. Imholt and J. Roberts and B.J. West. Solar turbulence in earths global and regional temperature anomalies. *Physical Review E*, 69(2): 026303, 2004.

[6] N. Scafetta and B.J. West. Solar flare intermittency and the Earths temperature anomalies. *Physical review letters*, 90(24): 248701, 2003.

[7] N. Scafetta and B.J. West. Estimated solar contribution to the global surface warming using the ACRIM TSI satellite composite. *Geophysical Research Letters*, 32(18), 2005. Wiley Online Library. [DOI: 10.1029/2005GL023849]

[8] N. Scafetta Global temperatures and sunspot numbers. Are they related? Yes, but non linearly. A reply to Gil-Alana et al.(2014). *Physica A: statistical Mechanics and its Applications*, 413: 329–342, 2014. Elsevier.

[9] C.K. Folland and A.W. Colman and D.M. Smith and O. Boucher and D.E. Parker and J.P. Vernier. High predictive skill of global surface temperature a year ahead. *Geophysical Research Letters*, 40(4): 761–767, 2013.

[10] J. Zhou and K.K. Tung. Deducing multidecadal anthropogenic global warming trends using multiple regression analysis. *Journal of the Atmospheric Sciences*, 70(1): 3–8, 2013.

[11] H. Hassani and X. Huang and R. Gupta and M. Ghodsi. Does sunspot numbers cause global temperatures? A reconsideration using non-parametric causality tests. *Physica A: Statistical Mechanics and its Applications*, 460: 54–65, 2016. Elsevier. [DOI:10.1016/j.physa.2016.04.013]

[12] R. Gupta and L. A. Gil-Alana and O. S. Yaya. Do sunspot numbers cause global temperatures? Evidence from a frequency domain causality test. *Applied Economics*, 47(8): 798–808, 2015.

[13] G. Sugihara and R. May and H. Ye and C. H. Hsieh and E. Deyle and M. Fogarty and S. Munch. Detecting causality in complex ecosystems. *Science*, 338(6106): 496–500, 2012.

[14] C.W. Granger. Investigating causal relations by econometric models and cross-spectral methods. *Econometrica: Journal of the Econometric Society*, 37(3): 424–438, 1969.

[15] C.A. Sims. Money, income, and causality. *The American Economic Review*, 62(4): 540–552, 1972.

[16] C. Hsiao. Autoregressive modelling and money-income causality detection. *Journal of Monetary Economics*, 7(1): 85–106, 1981.

[17] C. A. Sims and J. H. Stock and M. W. Watson. Inference in linear time series models with some unit roots. *Econometrica: Journal of the Econometric Society*, 58(1): 113–144, 1990.

[18] H. Y. Toda and P. C. Phillips. Vector autoregressions and causality. *Econometrica: Journal of the Econometric Society*, 61(6): 1367–1393, 1993.

[19] H. Y. Toda and T. Yamamoto. Statistical inference in vector autoregressions with possibly integrated processes. *Journal of Econometrics*, 66(1): 225–250, 1995.

[20] J. Geweke. Measurement of linear dependence and feedback between multiple time series. *Journal of the American Statistical Association*, 77: 304–324, 1982.

[21] C. Ciner. Eurocurrency interest rate linkages: A frequency domain analysis. *Review of Economics and Finance*, 20(4): 498–505, 2011.

[22] J. Breitung and B. Candelon. Testing for short- and long-run causality: A frequency-domain approach. *Journal of Econometrics*, 132: 363–378, 2006.

[23] E. Deyle and M. Fogarty and C. Hsieh and L. Kaufman and A. MacCall and S. Munch and C. Perretti and H. Ye and G. Sugihara. Predicting climate effects on Pacific sardine. *Proceedings of the National Academy of Sciences*, 110(16): 6430–435, 2013.

[24] H. Ye and E. Deyle and L. Gilarranz and G. Sugihara. Distinguishing time-delayed causal interactions using convergent cross mapping. *Scientific Reports*, 5, 2015.

[25] A. T. Clark and H. Ye and F. Isbell and E. Deyle and J. Cowles and G. Tilman and G. Sugihara. Spatial convergent cross mapping to detect causal relationships from short time series. *Ecology*, 96(5): 1174–1181, 2015.

[26] G. Sugihara and R. May. Nonlinear forecasting as a way of distinguishing chaos from measurement error in time series. *Nature*, 344(6268): 734–741, 1990.

[27] F. Takens. Detecting strange attractors in turbulence Dynamical Systems and Turbulence. *Dynamic Systems and Turbulence*, 898: 366–381, 1981.

[28] Goddard Institute for Space Studies (GISS). Available at: [http://data.giss.nasa.gov/gistemp]

[29] Solar Influences Data Analysis Centre (SIDC). Available at: [http://www.sidc.be/sunspot-data]

[30] J. Bai and P. Perron. Computation and analysis of multiple structural change models. *Journal of Applied Econometrics*, 18(1): 1–22, 2003.

[31] T. Alexandrov and S. Bianconcini and E.B. Dagum and P. Maass and T.S. McElroy. A review of some modern approaches to the problem of trend extraction. *Econometric Reviews*, 31(6): 593–624, 2012.

[32] H. Hassani. Singular spectrum analysis: methodology and comparison. *Journal of Data Science*, 5(2): 239–257, 2007.

[33] D. S. Broomhead and G. P. King. Extracting qualitative dynamics from experimental data. *Physica D: Nonlinear Phenomena*, 20(2):217–236, 1986.

[34] N. Golyandina, V. Nekrutkin, and A. Zhigljavsky. *Analysis of time series structure: SSA and related techniques.* CRC Press, 2010.

[35] D. Danilov and A. Zhigljavsky. Principal components of time series: the caterpillar method. *St. Petersburg: University of St. Petersburg*, pages 1–307, 1997.

[36] H. Hassani and S. Heravi and A. Zhigljavsky. Forecasting european industrial production with singular spectrum analysis. *International Journal of Forecasting*, 25(1): 103–118, 2009.

[37] H. Hassani and D. Thomakos. A review on singular spectrum analysis for economic and financial time series. *Statistics and its Interface*, 3(3): 377–397, 2010.

[38] H. Hassani and A. Zhigljavsky and K. Patterson and A. Soofi. A comprehensive causality test based on the singular spectrum analysis. *Causality in Science*, 379–406, 2010.

[39] H. Hassani and A. Dionisio and M. Ghodsi. The effect of noise reduction in measuring the linear and nonlinear dependency of financial markets. *Nonlinear Analysis: Real World Applications*, 11(1): 492–502, 2010.

[40] H. Hassani and S. Heravi and A. Zhigljavsky. Forecasting UK industrial production with multivariate singular spectrum analysis. *Journal of Forecasting*, 32(5): 395–408, 2013.

[41] H. Hassani and A. S. Soofi and A. Zhigljavsky. Predicting inflation dynamics with singular spectrum analysis. *Journal of the Royal Statistical Society: Series A (Statistics in Society)*, 176(3): 743–760, 2013.

[42] H. Hassani and R. Mahmoudvand. Multivariate singular spectrum analysis: A general view and new vector forecasting approach. *International Journal of Energy and Statistics*, 1(01): 55–83, 2013.